# TRANSVERSE EFFECTS DUE TO VACUUM MIRROR OF RF GUN

M. Dohlus, I. Zagorodnov#, DESY, Hamburg, Germany
M. Krasilnikov, DESY, Zeuthen, Germany
E. Gjonaj, S. Schnepp, TU Darmstadt, Germany.

*Abstract*

The transverse kick due to the vacuum mirror in the RF gun can negatively affect the beam emittance. In this contribution we estimate numerically and analytically the transverse wake function of the European XFEL RF gun and apply it in beam dynamics studies of the transverse phase space.

## INTRODUCTION

An electron beam with low emittance and high peak current is required in the European Free Electron Laser [1]. To meet these requirements, a laser-driven photocathode radio frequency (RF) gun has been designed and studied both experimentally and theoretically at DESY. The vacuum mirror of the laser is a main source of the transverse kick on the axis. It could disturb an emmitance compensation mechanism of the gun [2] considerably. In this contribution we estimate numerically and analytically the transverse kick due to the mirror and apply it in beam dynamics studies of the transverse phase space. The codes ECHO [3] and PBCI [4] are used to calculate the kick. The code ASTRA [5] is used for beam tracking.

## TRANSVERSE WAKE FUNCTION

### *Geometry of the vacuum mirror and the beam parameters*

The geometry and the main dimensions of the vacuum mirror are shown in Fig. 1.

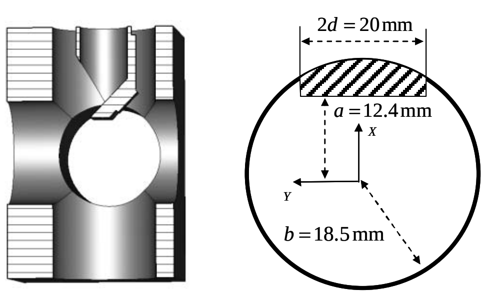


Figure 1: The mirror cross-sections.

The mirror has a complicated three dimensional shape, which was used in numerical simulations. The bunch length at the position of the mirror is about of $\sigma = 2$ mm with a transverse size of about 2.6 mm.

### *Analytical estimation of the wake function*

The parameters of the mirror and of the beam fulfill the relations $\sigma \ll a$, $L \ll a^2/\sigma$, where $L$ is the length of the mirror. Hence, we can simplify the model to a thin iris and use the optical approximation [6] to calculate the wake function.

The result for a source particle at position $x_s$ and a witness particle at position $x_w$ reads

$$k_x(x_s, x_w) = k_x(0,0) + k_x^D x_s + k_x^Q x_w,$$

$$k_x(0,0) = \frac{Z_0 c}{4ab^2\pi^2}\left[\left(b^2 - 2a^2\right)\alpha + ad\left(1 + \ln\frac{b^2}{B}\right)\right],$$

$$k_x^D = A\left[\begin{array}{l} ab^4 d - 4a^3 d^3 + b^4 d^2 \alpha - \\ a^2\left(2d^3 Q + b^4 \beta + b^2 d\left(Q - 4d\left(a + \beta\right)\right)\right)\end{array}\right],$$

$$k_x^Q = \frac{A}{B}\left[\begin{array}{l} ad\left(b^4\left(d^2 - a^2\right) + aB\left(b^2 + 6d^2\right)Q\right) + \\ B\left(d^2\alpha\left(b^4 - 8a^4\right) + a^2\beta\left(b^4 - 8d^4\right)\right)\end{array}\right],$$

$$\alpha = \arctan\left(\frac{d}{a}\right), \beta = \operatorname{arccot}\left(\frac{d}{Q}\right),$$

$$Q = \sqrt{b^2 - d^2}, B = a^2 + b^2, A = \frac{Z_0 c}{8a^2 b^4 d^2 \pi^2}.$$

The wake function of the point charge has the form

$$w_x(s, x_s, x_w) = 2\theta(s) k_x(x_s, x_w),$$

where $\theta(s)$ is a Heaviside function.

The wake potential for an arbitrary bunch profile $\lambda(s)$ can be found as

$$W_x(s) = 2k_x \Lambda(s), \qquad \Lambda(s) = \int_{-\infty}^{s} \lambda(s') ds'. \qquad (1)$$

In order to check the above analytical results we have calculated the kick of the thin iris for a bunch with an RMS length $\sigma = 0.5$ mm. The results are shown in Table 1. The analytical result does not depend on the bunch length $\sigma$.

Table 1: Kick for iris and σ=0.5 mm

| | $k_x(0,0)$, V/pC | $k_x^D$, V/pC/m | $k_x^Q$, V/pC/m |
|---|---|---|---|
| Analytical | 0.124 | 13.1 | 12.1 |
| Numerical | 0.120 | 13.1 | 11.6 |

#igor.zagorodnov@desy.de

### *Numerically calculated wakes*

The kick for the Gaussian pencil beam of the real mirror geometry was cross-checked with the codes PBCI and ECHO. The calculated wakes are shown in Fig.2.

Table 2: Kick for mirror and σ=2 mm

| | $k_x(0,0)$, V/pC | $k_x^D$, V/pC/m | $k_x^Q$, V/pC/m |
|---|---|---|---|
| Analytical | 0.12 | 13 | 12 |
| Numerical | 0.08 | 24 | 7.5 |

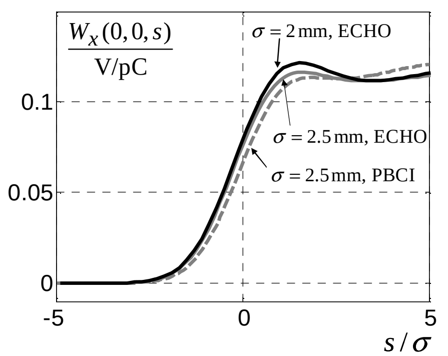


Figure 2: The transverse wakes of Gaussian bunches.

Table 2 compares the numerical and analytical results. We see that the simple analytical model overestimates the kick on the axis $k_x(0,0)$, but underestimates the term $k_x^D$.

## EMITTANCE GROWTH

### *Layout of the injector section and beam parameters*

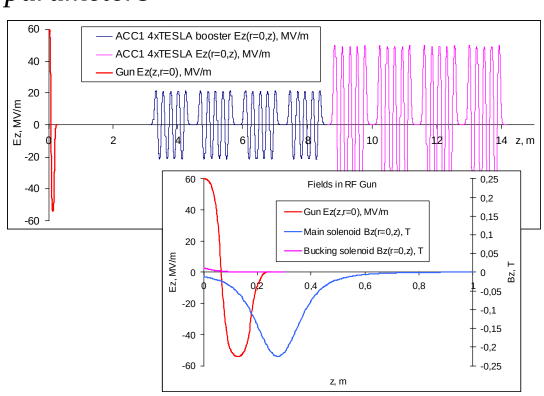


Figure 3: The longitudinal electric field on the axis.

The RF gun consists of 1,5-cell L-band cavity (1,3GHz), main solenoid centered at z=0.276 m and has -0.2247 T peak field. Magnetic field at the cathode is compensated by a bucking solenoid. The first four TESLA cavities of the first cryomodule (ACC1) with applied $E_{max}$=21.5 MV/m are used as a booster, the second half of the ACC1 with $E_{max}$=50 MV/m provides further beam acceleration. The axial field profile in the photo injector is shown in Fig.3. The temporal cathode laser profile is chosen to be a flat-top with 20 ps FWHM and 2 ps rise/fall time.

A radially homogeneous transverse laser distribution with 0.44 mm rms size has been used for ASTRA simulations involving 100000 macroparticles. Tracking of 1 nC electron bunch through the photo injector results in the projected rms beam emittance of 2.156 mm*mrad at the position of the vacuum mirror (z=62 cm).

The bunch shape at this position obtained from an ASTRA simulation with the charge $Q = 1\,\text{nC}$ is shown in Fig.4. Additionally this figure presents the wake potential calculated from Eq.(1) for $k_x(0,0) = 0.08$ kV/nC.

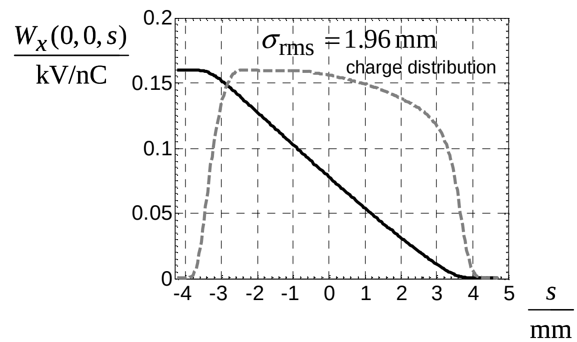


Figure 4: The bunch shape and the transverse wake potential.

### *Analytical estimation of the emittance growth*

The kick at the mirror is given as

$$\Delta x'(s) = \frac{\Delta p_x}{p_z} = \frac{eQW_x(s)}{\beta_z^2 E_{kin}} = 2S\Lambda(s)\,, \quad S = \frac{eQk_x}{\beta_z^2 E_{kin}}\,.$$

Let us consider a transverse Gaussian particle distribution

$$\rho_0(x,x',s) = \frac{1}{2\pi\varepsilon_{0x}} \exp\left(-\frac{\gamma x^2 + 2\alpha x x' + \beta x'^2}{2\varepsilon_{0x}}\right)\lambda(s)$$

with an arbitrary longitudinal profile $\lambda(s)$.

After the kick the distribution has the form

$$\rho = \frac{\lambda(s)}{2\pi\varepsilon_{0x}} \exp\left(-\frac{\gamma x^2 + 2\alpha x(x' + \Delta x'(s)) + \beta(x' + \Delta x'(s))^2}{2\varepsilon_{0x}}\right).$$

The projected distribution does not depend on the $\lambda(s)$

$$\bar{\rho} = \int_{-\infty}^{\infty} \rho(x,x',s)ds = \int_0^1 \frac{1}{2\pi\varepsilon_{0x}} e^{-\frac{\gamma x^2 + 2\alpha x(x'+2S\Lambda) + \beta(x'+2S\Lambda)^2}{2\varepsilon_{0x}}} d\Lambda =$$

$$= \frac{Erf\left(\frac{x\alpha + (2S + x')\beta}{\sigma_{0x}\sqrt{2}}\right) - Erf\left(\frac{x\alpha + x'\beta}{\sigma_{0x}\sqrt{2}}\right)}{4\sqrt{2\pi}S\sigma_{0x}} e^{-\frac{x^2}{2\sigma_{0x}{}^2}}\,,$$

where $\sigma_{0x} = \sqrt{\varepsilon_{0x}\beta}$ .

The projected emittance can be calculated analytically

$$\varepsilon_x = \sqrt{\langle x^2\rangle\langle x'^2\rangle - \langle xx'\rangle} = \sqrt{\varepsilon_{0x}{}^2 + S^2\frac{\varepsilon_{0x}\beta}{3}} \approx \varepsilon_{0x} + S^2\frac{\beta}{6}$$

Hence, the relative emittance growth reads

$$\frac{\varepsilon_x - \varepsilon_{0x}}{\varepsilon_{0x}} = \sqrt{1 + S^2\frac{\beta}{3\varepsilon_{0x}}} - 1 \approx S^2\frac{\beta}{6\varepsilon_{0x}}. \qquad (2)$$

From ASTRA simulations for bunches with $Q = 1\,\text{nC}$ we have found at position of the mirror

$$\frac{E_{kin}}{e} = 6.6\ \text{MeV}\ , \beta = 8.4\ \text{m}\ , \gamma\varepsilon_{0x} = 2.156\ \text{mm}\times\text{mrad}\ .$$

Hence, for $k_x = 0.124$ kV/nC the analytical estimation of the emittance growth gives

$$\frac{\varepsilon_x - \varepsilon_{0x}}{\varepsilon_{0x}} = 0.3\%\ .$$

### *Numerical results for the emittance growth*

The above estimation is too optimistic as it does not take into account that the time-dependent character of the kick can disturb the emittance compensation process. In order to check it we have done beam dynamic simulations up to 15 meter after the cathode. The simulations were done as follows: the particle distribution is tracked in ASTRA from the cathode up to the position of the mirror. There, the transverse wake potential of the mirror is applied, and the new distribution is tracked up to the end of the cryomodule. Fig.5 presents the emittance of the bunch after the kick. The black line with the lowest values shows the emittance without any kick. The gray curves describe the emittance when the kick is applied.

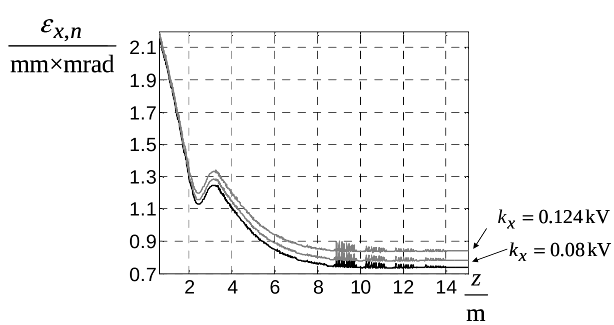


Figure 5: The emittance along the injector section.

The emittance growth at position of the mirror and after the cryomodule is presented in Table 3. A much more sophisticated tracking with PBCI 3D field solver [4] has shown 0.5% of emittance growth in the vicinity of the mirror. It agrees well with the above analytical estimation and the first number of Table 3.

The above numbers describe a situation when the bunch moves on the axis. But we can use the results of ECHO simulations from Table 2 for the terms $k_x^D$, $k_x^Q$ to estimate the kick and the emittance growth when the bunch moves with an offset. Eq.2 suggests a quadratic dependence of the emittance growth on the kick:

$$\frac{\varepsilon_x - \varepsilon_{0x}}{\varepsilon_{0x}} = O(k_x{}^2)$$

Table 3: Emittance growth in %

| position, m | $k_x(0,0)$= =0.08 kV | $k_x(0,0)$= =0.124 kV |
|---|---|---|
| 0.62 | 0.6 | 1.4 |
| 15 | 6 | 14 |

We could apply this dependence and extrapolate the data of Table 3 to the case of the offset. Fig.6 presents such a crude estimation based on the straightforward extrapolation of the final result for $k_x(0,0) = 0.08$ kV.

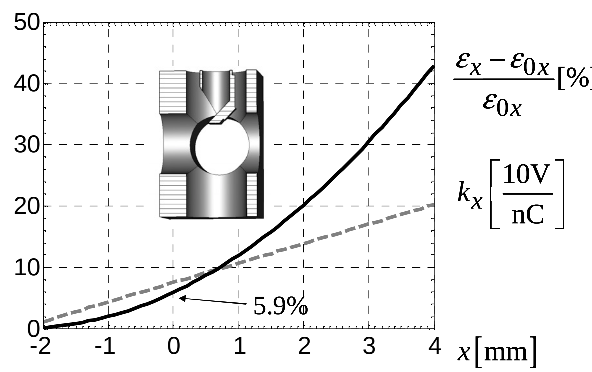


Figure 6: Emittance growth vs. bunch offset.

For the bunch with an offset of 2 mm the emittance growth could be about 20%.

In this simulation we have used rotationally symmetric space charge solver of ASTRA and we do not try to optimize the parameters of the gun to correct emittance compensation process. Hence, we consider this estimation as quite conservative.

To bring the model more closely to the reality we are going to do more elaborated tracking with the PBCI 3D field solver. As the next step a fully self consistent 3D simulation with a Particle-In-Cell code is planned.

## REFERENCES

[1] M. Altarelli et al, The European X-Ray Free Electron Laser, DESY 2006-097 (2007).
[2] B.E. Carlsten, NIM A285 (1989) 313.
[3] I. Zagorodnov, T. Weiland, Phys. Rev. STAB, 8 (2005) 042001.
[4] E. Gjonaj et al, New J. Phys. 8 (2006) 285.
[5] K. Floettmann, ASTRA User's Manual, http://www.desy.de/~mpyflo/Astra_dokumentation.
[6] G. Stupakov, K. Bane, I. Zagorodnov, Phys. Rev. STAB, 10 (2007) 054401.